Southern Ocean Isopycnal Mixing and Ventilation Changes Driven by Winds

Ryan Abernathey[1] and David Ferreira,[2]

[1]Lamont Doherty Earth Observatory of Columbia University, Palisades, New York, USA.

[2]Department of Meteorology, University of Reading, Reading, UK.

Observed and predicted changes in the strength of the westerly winds blowing over the Southern Ocean have motivated a number of studies of the response of the Antarctic Circumpolar Current and Southern Ocean Meridional Overturning Circulation (MOC) to wind perturbations and led to the discovery of the"eddy-compensation" regime, wherein the MOC becomes insensitive to wind changes. In addition to the MOC, tracer transport also depends on mixing processes. Here we show, in a high-resolution process model, that isopycnal mixing by mesoscale eddies is strongly dependent on the wind strength. This dependence can be explained by mixing-length theory and is driven by increases in eddy kinetic energy; the mixing length does not change strongly in our simulation. Simulation of a passive ventilation tracer (analogous to CFCs or anthropogenic CO_2) demonstrates that variations in tracer uptake across experiments are dominated by changes in isopycnal mixing, rather than changes in the MOC. We argue that, to properly understand tracer uptake under different wind-forcing scenarios, the sensitivity of isopycnal mixing to winds must be accounted for.

1. Introduction

The steeply sloped isopycnal surfaces of the Southern Ocean, which outcrop at the surface and rapidly deepen across the Antarctic Circumpolar Current (ACC), provide an adiabatic pathway for exchange between the atmosphere and deep ocean. For this reason, the Southern Ocean is believed to play a central role in regulating the ocean-atmosphere exchange of carbon, heat and other tracers [*Broecker*, 1997; *Caldeira and Duffy*, 2000; *Sabine et al.*, 2004; *Gille*, 2008; *Anderson et al.*, 2009; *Khatiwala et al.*, 2009]. The Southern Ocean is already a major region of uptake of anthropogenic carbon and heat, and the future evolution of this carbon sink is one of the uncertainties in forecasts of future climate change [*Le Quéré et al.*, 2009]. A compelling hypothesis is that interactions between wind forcing, Southern Ocean circulation, and atmospheric carbon lead to important climate feedbacks with the potential to regulate both glacial cycles and anthropogenic climate change [*Toggweiler and Russell*, 2008; *Toggweiler*, 2009]. However, the puzzle posed recently by *Landschützer et al.* [2015] (i.e. that Southern Ocean CO_2 uptake has increased over the last decade, in contrast with previous estimates for the 80s and 90s [*Le Quéré et al.*, 2007]) highlights our incomplete understanding of the sensitivity of the ventilation process.

Southern Ocean ventilation involves both advective and diffusive transport, and mesoscale eddies participate in both aspects [*Lee et al.*, 1997, 2007]. The advective part is closely tied to the Meridional Overturning Circulation (MOC) [*Lumpkin and Speer*, 2007; *Marshall and Speer*, 2012], and ocean circulation theory suggests that the Southern Ocean westerly winds control the strength of the upwelling branch of the MOC [*Gnanadesikan*, 1999; *Marshall and Radko*, 2003; *Nikurashin and Vallis*, 2012; *Rintoul and Naveira Garabato*, 2013]. A large amount of recent research has probed the nature of this dependence, and, in particular, the role played by mesoscale eddies in advective transport. While some coarse resolution ocean models do demonstrate strong MOC dependence on winds, more realistic higher resolution models exhibit so-called "eddy compensation," wherein changes in eddy-induced overturning largely cancel changes in wind-driven overturning [*Hallberg and Gnanadesikan*, 2006; *Spence et al.*, 2009; *Farneti et al.*, 2010; *Abernathey et al.*, 2011; *Farneti and Gent*, 2011; *Meredith et al.*, 2012; *Farneti et al.*, 2015; *Gent*, 2015]. This behavior is compatible with hydrographic observations showing that isopycnal slopes in the Southern Ocean have not significantly steepened over the past decades despite the substantial intensification of the westerlies over the same period, implying that eddy-induced vertical advection has compensated for changes in Ekman pumping [*Böning et al.*, 2008]. We therefore have some evidence from both observations and models that, in the present climate, the residual MOC is not as strongly sensitive to westerly wind changes as Ekman theory alone would suggest, although the sensitivity of the real ocean has not been measured and remains open to debate [see *Rintoul and Naveira Garabato*, 2013]. At the same time, there are indications that Southern Ocean ventilation has changed in recent decades. Using CFC data, *Waugh et al.* [2013] demonstrated a decrease in the age of subantarctic mode water and an increase in the age of circumpolar deep water [see also *Waugh*, 2014].

For tracers other than density, it is well known that eddy-diffusive transport along isopycnals can be as important as advection by the MOC, and, depending on the timescales and tracer gradients, can act in opposition to advection [*Lee et al.*, 1997; *Lee and Williams*, 2000; *Lee et al.*, 2007]. Indeed, recent studies with a comprehensive climate model (in which eddy mixing is parameterized following *Redi* 1982) have demonstrated that isopycnal diffusivity exerts a strong control over Antarctic sea ice [*Pradal and Gnanadesikan*, 2014], trace elements [*Gnanadesikan et al.*, 2014], anthropogenic carbon uptake [*Gnanadesikan et al.*, 2015], and carbon pumps (Gnanadesikan et al., submitted manuscript). Despite the dozens of papers on the advective response of mesoscale eddies to wind changes, there has been no investigation into the *changes* in isopycnal mixing which occur in response to wind changes in eddy-resolving models. This is the goal of our paper.

In this study, we use an eddy-resolving numerical model of an idealized circumpolar channel to demonstrate that isopycnal mixing, unlike the MOC, is strongly sensitive to wind changes. This analysis is enabled by a tracer-based technique which permits the explicit diagnosis of isopycnal diffusivity as a function of depth and latitude [*Nakamura*, 1996]. We show how mixing-length theory can be used to explain the sensitivity of isopycnal mixing to the winds, via the eddy-kinetic-energy dependence on wind power input. We then demonstrate that these changes in isopycnal mixing lead to significant differences in the uptake of a transient ventilation tracer (analogous to tracers such as anthropogenic CO_2 or CFCs).

2. Model Description

The simulations are designed to qualitatively resemble the ACC in ways relevant for mixing and ventilation. The model set-up is identical to that used by *Abernathey et al.* [2011], *Hill et al.* [2012], and, *Abernathey et al.* [2013], which the reader should consult for further details. The code uses the MITgcm [*Marshall et al.*, 1997a, b] to solve the Boussinesq primitive equations. A linear equation of state with no salinity is employed. The domain is a zonally reentrant channel on a β-plane, 1000 km x 2000 km x 2985 m. Forcing consists of zonally symmetric zonal wind stress and fixed heat flux. The wind stress forcing is a sinusoid which peaks in the center of the domain with a maximum value of τ_0 (to be varied as described below). The heat flux contains alternating regions of cooling, heating, and cooling, with an amplitude of 10 W m^{-2}. Spurious numerical diffusion is minimized through the use of a second-order-moment advection scheme [*Prather*, 1986], resulting in an effective diapycnal diffusivity of about 10^{-5} m^2 s^{-1} [*Hill et al.*, 2012]. Resolution is 5 km in the horizontal with 30 unevenly spaced vertical levels. With a Rossby radius of approx. 20 km, this model can be considered "eddy resolving."

The northern boundary is a sponge layer in which the temperature is relaxed to an exponential stratification profile with an e-folding scale of 1000 m, similar to observed profiles in the Southern Ocean [*Karsten and Marshall*, 2002]. The presence of the sponge layer, together with the applied pattern of heating and cooling, allows a nonzero residual overturning, qualitatively resembling the real Southern Ocean [see e.g. *Marshall and Radko*, 2003; *Lumpkin and Speer*, 2007], to emerge.

To explore the sensitivity of the system to wind stress, we conduct three experiments with different values of τ_0: 0.1, 0.2, and 0.3 N m^{-2}. This range represents a strong yet plausible variation in Southern hemisphere westerly winds over climate timescales. As shown in *Abernathey et al.* [2011], with the fixed-flux boundary condition employed here, the residual MOC (averged in density rather than depth space) depends rather weakly on the winds compared to the Ekman / Eulerian-mean overturning: the upper cell increases from about 0.4 Sv to 0.6 Sv as the winds (and associated Ekman transport) are tripled.

Although the model is highly idealized in its geometry, the eddy statistics and transports in the $\tau_0 = 0.1$ N m^{-2} experiment are realistic. The surface eddy kinetic energy (EKE) of roughly 300 cm^2 s^{-2} is comparable to that observed by satellite altimetry in the Southern Ocean [*Stammer*, 1997], and the decay of EKE in the vertical has a similar profile to more realistic global models [*Vollmer and Eden*, 2013]. If the 1000 km width is rescaled to the zonal extent of the full ocean, the residual MOC transport would be 12 Sv, well within the observational error bars [*Lumpkin and Speer*, 2007; *Mazloff et al.*, 2010]. Likewise, the eddy isopycnal diffusivities (described further below) have significant spatial variability and reach a maximum magnitude of approx. 4000 m^2 s^{-1}, similar to estimates from more realistic models [*Abernathey et al.*, 2010; *Lee et al.*, 2007].

The most unrealistic aspect of the model is its zonal symmetry. In the real Southern Ocean, eddy activity and mixing are concentrated around topographic hotspots [*Treguier and McWilliams*, 1990; *Naveira-Garabato et al.*, 2011; *Thompson and Sallée*, 2012]. We use a zonally symmetric model to isolate the fundamental parametric sensitivity of isopycnal mixing to external forcing, and because isopycnal diffusivty is much harder to quantify without zonal averaging due to the presence of non-local eddy fluxes. *Abernathey and Cessi* [2014] examined the interaction between mesoscale eddies and topography in similar idealized simulations. They concluded that topography enhances the overall efficiency of eddy mixing, but that eddy kinetic energy remains highly sensitive to winds. Furthermore, they showed how the additional "stationary eddy" fluxes that arise due to topographic meanders are only possible due to transient eddies, and that a transformation to "streamwise" coordinates which follow the topographically induced meanders can remove the stationary component [*de Szoeke and Levine*, 1981; *Marshall et al.*, 1993; *Viebahn and Eden*, 2012]. We therefore expect that our results here will apply qualitatively to more realistic geometries, although the mixing would be more localized near topography.

3. Isopycnal Effective Diffusivity

We diagnose isopycnal mixing rates using the modified-Lagrangian-mean effective diffusivity framework of *Nakamura* [1996] [see also *Haynes and Shuckburgh*, 2000; *Shuckburgh and Haynes*, 2003; *Marshall et al.*, 2006; *Abernathey et al.*, 2010]. *Abernathey et al.* [2013] used this model configuration to conduct a detailed study of the spatial structure of isopycnal mixing and compare different methods of diagnosing isopycnal diffusivity, including Lagrangian diffusivity from simulated particles, passive tracer releases, and inversion from the eddy flux of potential vorticity. They concluded that, when properly executed, the different methods all produce a consistent estimate of the magnitude and spatial structure of isopycnal mixing.

Here, for simplicity, we focus on the effective diffusivity of *Nakamura* [1996]. It is computed by releasing a passive tracer with an initial meridional gradient, allowing it to be stirred by the model velocity field, and quantifying the resulting fine structure that is produced. The effective diffusivity is defined as:

$$K_{eff} = \kappa \frac{L_e^2}{L_{min}^2} \tag{1}$$

where κ is the grid-scale horizontal diffusivity, L_e is the "equivalent length" of a filamented tracer contour, and L_{min} is the minimum possible length of the contour (here equal to 1000 km, the length of the domain). L_e is diagnosed, as described in *Nakamura* [1996], through a robust numerical method involving area integrals over the instantaneous tracer gradient. In the high Peclet-number regime considered here, K_{eff} becomes independent of κ, leading to a converged estimate of mixing rates [*Marshall et al.*, 2006].

Following the detailed procedure of *Abernathey et al.* [2013] for a robust estimate of K_{eff}, the passive tracer is released and allowed to evolve for two years, with snapshots output every month. At each snapshot, the tracer is interpolated to isopycnals and K_{eff} is calculated following (1). Five such two-year periods are repeated to produce an ensemble average of K_{eff} for each wind magnitude.

The results of the K_{eff} calculation are shown in Fig. 1, as functions of latitude and density (the native coordinate for the calculation, top row) and also latitude and depth (second row). The spatial structure of K_{eff} matches a now-well-understood paradigm, with reduced values near the surface and bottom and a maximum near 1000 m depth [*Abernathey et al.*, 2010; *Naveira-Garabato et al.*, 2011]. This spatial structure can be explained using mixing-length arguments which account for the mixing-suppression effect of eddy propagation relative to the mean flow [*Ferrari and Nikurashin*, 2010; *Klocker et al.*, 2012a, b; *Klocker and Abernathey*, 2014]. Specifically,

$$K_{eff} \simeq \Gamma v_{rms} L_{mix} \tag{2}$$

where Γ is an $O(1)$ constant called mixing efficiency, v_{rms} is the root-mean-square eddy velocity, and L_{mix} is the mixing length, related to the eddy size and the eddy phase speed relative to the mean flow.

The magnitude of K_{eff} clearly increases with increasing winds, while its spatial structure remains mostly unchanged. These changes are driven almost entirely by changes in EKE. As shown in Fig. 1, EKE also increases strongly with winds. We also calculate an effective mixing length L_{mix} by inverting Eq. (2), using $\Gamma = 0.35$ and $v_{rms}=\sqrt{2EKE}$ [*Klocker and Abernathey*, 2014]. The effective mixing length remains roughly constant in magnitude and spatial structure as the winds change strength (Fig. 1, bottom row). The spatial structure of L_{mix} is consistent with the mixing-suppression model of *Ferrari and Nikurashin* [2010], in which eddy phase propagation relative to the (spatially variable) zonal mean flow suppresses the mixing rate. The lack of sensitivity of L_{mix} to the winds shows that such effects themselves do not depend strongly on winds in this scenario; both eddy propagation and zonal mean flow change relatively little.

The strong dependence of EKE on winds can be understood based on the mechanical energy balance. Wind work is the primary source of energy for the ocean, and there is strong observational evidence that bottom drag is a dominant mechanism for mesoscale energy dissipation [*Sen et al.*, 2008; *Wright et al.*, 2012, 2013]. If the wind forcing increases, the eddy dissipation must also increase, which requires an increase in eddy amplitude. Specifically, with the linear bottom drag employed in this model, one expects a linear dependence of EKE on wind stress [*Cessi*, 2008; *Abernathey et al.*, 2011]. If L_{mix} changes weakly, this implies $K_{eff} \propto \tau_0^{1/2}$. Other types of bottom drag than linear (e.g. quadratic or lee wave) would have quantitatively different, but qualitatively similar, scalings.

We illustrate these scalings in Fig. 2 by plotting EKE, L_{mix}, and K_{eff}, averaged over a small mid-depth region indicated by the box in Fig. 1. (Using a small region avoids artifacts arising from compensatory spatial correlations of EKE and L_{mix}.) Fig. 2 shows that EKE does indeed have a linear relationship with τ_0, L_{mix} remains constant, and K_{eff} increases roughly proportionally to $\tau_0^{1/2}$. Log-linear fits of the points in Fig. 2 give a scaling exponent of 1.0 for EKE and 0.57 for K_{eff}. Similar scaling holds at other points in the domain.

4. Transient Ventilation Tracer

Isopycnal mixing has a limited effect on the physical circulation because it does not affect density. However, it has a strong effect on other tracers. To illustrate this, we simulate an idealized ventilation tracer, meant as a crude analog of observed passive tracers such as CFCs or anthropogenic CO_2.

At the surface, the ventilation tracer is forced by a relaxation to a value of 1 unit/m^3 (with a restoring timescale of 6 hours), the simplest representation of air-sea exchanges with a large atmospheric reservoir. The ventilation tracer is also restored to zero in the northern boundary sponge layer, effectively assuming that the ventilation tracer leaves the domain at the northern boundary. The tracer is mixed near the surface by the mixed layer scheme, but no other explicit mixing is applied (i.e. it is treated the same as temperature). Note that the advection scheme of *Prather* [1986] is also used on the tracer, which therefore experiences a very low numerical diapycnal mixing [*Hill et al.*, 2012]. Thus, in the ocean interior, the ventilation tracer is, to a good approximation, advected passively by the turbulent flow and conserved on isopycnals.

The tracer is initialized uniformly to zero and its transient evolution simulated over 10 years; results are summarized in Fig. 3. It is readily seen that the uptake of tracer is much larger with stronger winds (top row). After 5 years, the tracer occupies the whole ventilated thermocline (above the 0.25°C isotherm) up to the Northern boundary for τ_0=0.3 N m^{-2}. For a weaker wind (0.1 N.m^{-2}), the tracer barely extends across the mid-channel in the ocean interior. Quantitatively, the total tracer uptake is about 50% times larger with τ_0=0.3 than 0.1 N.m^{-2} after 5 years (bottom left).

Local differences are also evident. The tracer uptake clearly follows the pattern of the residual-mean overturning with maximum uptake along isotherms associated with the downwelling branches. However, net uptake of tracer is also seen on isotherms with upwelling. On these isotherms, the spreading of the tracer is due to isopycnal mixing (recall the very small diapycnal mixing), working against the upwelling flow that brings tracer-free water parcels upwards. We emphasize here that, on the isotherms with net upwelling, the upwelling rate *increases* with increasing winds. Because the system is in an eddy-compensated regime, changes in upwelling rates are not as large as those expected from changes in the wind-driven circulation alone [see *Abernathey et al.*, 2011], but are significant nonetheless. On the isotherm of maximum upwelling (1.5, 1.1 and 0.9 °C), the upwelling flows (along the isotherm) are 7.8 cm s^{-1}, 11.4 cm s^{-1}, and 15.1 cm s^{-1} for τ_0=0.1, 0.2, and 0.3 N.m^{-2}, respectively.

The advance of the 0.1 unit m^3 tracer contour along the isotherm of maximum upwelling is shown in Fig. 3 (bottom right). We observe that the ventilation tracer penetrates much faster into the ocean interior, against the upwelling flow, for larger winds. This is a key point: despite the increased upwelling, the tracer uptake is larger with increased winds; changes in isopycnal mixing dominate over changes of the residual MOC.

Our ventilation tracer is idealized (e.g. solubility effects have been neglected) and has a fast air-sea flux time scale, and cannot readily be used to estimate the wind effect on the uptake of observed tracers [see discussion in *Ito et al.*, 2004]. However, it illustrates that tracer uptake does increase with increasing winds (globally and locally) mainly through the effects of intensified isopycnal mixing. These results are compatible with *Gnanadesikan et al.* [2015], who found that increasing the isopycnal mixing coefficient in a coarse-resolution model led to increased uptake of CO_2 by the ocean.

5. Discussion and Conclusions

The discussion of the Southern Ocean response to wind changes (motivated by recent observed changes due to ozone depletion and CO_2 emissions or by a paleoclimate context) has mostly been concerned with the response of the strength of the ACC and MOC. Early suggestions were that changes in the MOC would scale with those of the wind-driven component and would be relatively large, with large impacts on the uptake of tracers such as anthropogenic CO_2 [*Toggweiler*, 2009; *Le Quéré et al.*, 2009]. Recent modeling studies [*Hallberg and Gnanadesikan*, 2006], backed up by theoretical arguments [*Abernathey et al.*, 2011] and observations [*Böning et al.*, 2008] suggest a much more moderate impact of winds on the residual-mean (or effective) MOC, accounting for the adjustment of the eddy-induced MOC to wind changes – the so-called "eddy compensation" regime [see also *Farneti et al.*, 2010; *Viebahn and Eden*, 2010; *Meredith et al.*, 2012; *Rintoul and Naveira Garabato*, 2013; *Farneti et al.*, 2015; *Gent*, 2015]. This emphasis on the *advective* component neglects the important role played by *diffusive* isopycnal eddy mixing in tracer transport [*Lee et al.*, 1997, 2007]. In the present study, we demonstrate for the first time that isopycnal mixing is strongly dependent on the strength of the westerly winds and, further, that this dependence leads to different rates of uptake of a transient ventilation tracer. More precisely, we illustrate that *changes* in the isopycnal mixing of a ventilation tracer can be large enough to overcome *changes* in advection.

Coarse resolution ocean climate models represent the advective and isopycnal mixing effects of mesoscale eddies through two separate parameterizations. The *Gent and McWilliams* [1990] parameterization provides an eddy-induced advection velocity whose strength is governed by the so-called "GM coefficient" K_{GM}, while the *Redi* [1982] parameterization provides along-isopycnal diffusion with diffusivity K_{Redi}. Although they both parameterize unresolved mesoscale turbulence, the relationship between these two coefficients is non-trivial [*Smith and Marshall*, 2009; *Abernathey et al.*, 2013]. Our K_{eff} calculations here are comparable to K_{Redi}, while the eddy transfer coefficients in *Abernathey et al.* [2011] were comparable to K_{GM}.

Because of its role in equilibrating the pycnocline and producing advective transport, the GM coefficient is crucial to properly reproducing eddy saturation in coarse-resolution models; *Farneti and Gent* [2011] showed that a coarse-resolution model with an interactive K_{GM} was able to better (but not perfectly) match the response of a high-resolution model, and an intercomparison of a large number of models with different treatments of K_{GM} by *Farneti et al.* [2015] reached the same conclusion. In fact, the eddy-saturation regime demands that the eddy-induced advection is strongly sensitive to wind changes, which, in the limit of small changes in isopycnal slopes, requires a large wind-dependence of K_{GM} [*Abernathey et al.*, 2011]. The present study shows that the isopycnal mixing coefficients are similarly sensitive to wind changes. Although K_{Redi} is not particularly relevant for eddy saturation or eddy compensation, it has a large impact on anthropogenic CO_2 uptake and biogeochemical cycles [*Gnanadesikan et al.*, 2015]. Nearly all coarse-resolution models employ a constant value of K_{Redi}, yet our experiments show that this parameter should in fact change under different forcing scenarios.

The recent work by *Landschützer et al.* [2015], showing an increased CO_2 uptake in the Southern Ocean since 2002, gives important context to our work. Their finding contrasts with expectations that the CO_2 sink was weakening in response to the strengthening of the Southern Hemisphere Westerly winds. Importantly, our results suggest that an increase in winds could drive *increased* CO_2 uptake in the Southern Ocean through changes in isopycnal mixing rates. Changes in ventilation rates of the Southern Ocean therefore constitute a climate feedback of indeterminate sign, depending on the dominance of advective or diffusive changes in response to wind changes. Our results demonstrate that a detailed understanding of the sensitivity of mesoscale eddy transports, advective and diffusive, to wind changes is crucial to resolving this problem.

Acknowledgments. R.A. acknowledges support from NSF grant OCE-1357133. Model setups, output data, and analysis code are all available on request.

References

Abernathey, R., J. Marshall, E. Shuckburgh, and M. Mazloff (2010), Enhancement of mesoscale eddy stirring at steering levels in the Southern Ocean, *J. Phys. Oceanogr.*, *40*, 170–185, doi:10.1175/2009JPO4201.1.

Abernathey, R., J. Marshall, and D. Ferreira (2011), The dependence of Southern Ocean meridional overturning on wind stress, *J. Phys. Oceanogr.*, *41*(12), 2261–2278, doi:10.1175/JPO-D-11-023.1.

Abernathey, R., D. Ferreira, and A. Klocker (2013), Diagnostics of isopycnal mixing in a circumpolar channel, *Ocean Modelling*, *72*, 1 – 16, doi:10.1016/j.ocemod.2013.07.004.

Abernathey, R. P., and P. Cessi (2014), Topographic enhancement of eddy efficiency in baroclinic equilibration, *J. Phys. Oceanogr.*, *44*, 2107–2126, doi:10.1175/JPO-D-14-0014.1.

Anderson, R. F., S. Ali, L. I. Bradtmiller, S. H. H. Nielsen, M. Q. Fleisher, B. E. Anderson, and L. H. Burckle (2009), Wind-driven upwelling in the Southern Ocean and the deglacial rise in atmospheric CO_2, *Science*, *323*, 1143–1150.

Böning, C. W., A. Dispert, M. Visbeck, S. R. Rintoul, and F. U. Schwarzkopf (2008), The response of the antarctic circumpolar current to recent climate change, *Nature Geoscience*, *1*, 864–870.

Broecker, W. S. (1997), Thermohaline circulation, the achilles heel of our climate system: Will man-made CO_2 upset the current balance?, *Science*, *278*(5343), 1582–1588.

Caldeira, K., and P. B. Duffy (2000), The role of the southern ocean in uptake and storage of anthropogenic carbon dioxide, *Science*, *287*(5453), 620–622.

Cessi, P. (2008), An energy-constrained parameterization of eddy buoyancy flux, *J. Phys. Oceanogr.*, *38*, 1807–1820.

de Szoeke, R. A., and M. D. Levine (1981), The advective flux of heat by mean geostrophic motions in the Southern Ocean, *Deep Sea Res.*, *28A*(10), 1057–1085.

Farneti, R., and P. R. Gent (2011), The effects of the eddy-induced advection coefficient in a coarse-resolution coupled climate model, *Ocean Modelling*, *39*(1), 135–145.

Farneti, R., T. L. Delworth, A. J. Rosati, S. M. Griffies, and F. Zeng (2010), The role of mesoscale eddies in the rectification of the Southern Ocean response to climate change, *J. Phys. Oceanogr.*, *40*, 1539–1558.

Farneti, R., et al. (2015), An assessment of Antarctic Circumpolar Current and Southern Ocean meridional overturning circulation during 1958–2007 in a suite of interannual core-II simulations, *Ocean Modelling*, *93*, 84-120.

Ferrari, R., and M. Nikurashin (2010), Suppression of eddy diffusivity across jets in the Southern Ocean, *J. Phys. Oceanogr.*, *40*, 1501–1519.

Gent, P. (2015), Effects of southern hemisphere wind changes on the amoc from models, *Annual Review of Marine Science.*

Gent, P., and J. McWilliams (1990), Isopycnal mixing in ocean circulation models, *J. Phys. Oceanogr.*, *20*, 150–155.

Gille, S. T. (2008), Decadal-scale temperature trends in the southern hemisphere ocean, *Journal of Climate*, *21*(18), 4749–4765.

Gnanadesikan, A. (1999), A simple predictive model for the structure of the oceanic pycnocline, *Science*, *283*, 2077–2079.

Gnanadesikan, A., R. Abernathey, and M.-A. Pradal (2014), Exploring the isopycnal mixing and helium-heat paradoxes in a suite of earth system models, *Ocean Science Discussions*, *11*(6), 2533–2567, doi:10.5194/osd-11-2533-201.

Gnanadesikan, A., M.-A. Pradal, and R. Abernathey (2015), Isopycnal mixing by mesoscale eddies significantly impacts oceanic anthropogenic carbon uptake, *Geophysical Research Letters*, *42*(11), 4249–4255, doi:10.1002/2015GL064100, 2015GL064100.

Hallberg, R., and A. Gnanadesikan (2006), The role of eddies in determining the structure and response of the wind-driven southern hemisphere overturning: Results from the modeling eddies in the souther ocean (meso) project, *J. Phys. Oceanogr.*, *36*, 2232–2252.

Haynes, P., and E. Shuckburgh (2000), Effective diffusivity as a diagnostic of atmospheric transport. part i: stratosphere, *J. Geophys. Res*, *105*, 22,777–22,794.

Hill, C., D. Ferreira, J.-M. Campin, J. Marshall, R. Abernathey, and N. Barrier (2012), Controlling spurious diapycnal mixing in eddy-resolving height-coordinate ocean models: Insights from virtual deliberate tracer release experiments, *Ocean Modelling*, *45-46*, 14–26, doi:10.1016/j.ocemod.2011.12.001.

Ito, T., J. Marshall, and M. Follows (2004), What controls the uptake of transient tracers in the southern ocean?, *Global biogeochemical cycles*, *18*(2).

Karsten, R. H., and J. Marshall (2002), Testing theories of the vertical stratification of the acc against observations, *Dyn. Atmos. Oceans*, *36*, 233–246.

Khatiwala, S., F. Primeau, and T. Hall (2009), Reconstruction of the history of anthropogenic CO_2 concentrations in the ocean, *Nature*, *462*(7271), 346–349.

Klocker, A., and R. Abernathey (2014), Global patterns of mesoscale eddy properties and diffusivities, *J. Phys. Oceanogr.*, *44*, 1030–1047, doi:10.1175/JPO-D-13-0159.1.

Klocker, A., R. Ferrari, and J. H. LaCasce (2012a), Estimating suppression of eddy mixing by mean flow, *J. Phys. Oceanogr.*, *9*, 1566–1576.

Klocker, A., R. Ferrari, J. H. LaCasce, and S. T. Merrifield (2012b), Reconciling float-based and tracer-based estimates of eddy diffusivities, *J. Marine Res.*, *70*(4), 569–602.

Landschützer, P., et al. (2015), The reinvigoration of the southern ocean carbon sink, *Science*, *349*, 1221–1224, doi:10.1126/science.aab2620.

Le Quéré, C., et al. (2007), Saturation of the southern ocean CO_2 sink due to recent climate change, *Science*, *316*, 1735–1738.

Le Quéré, C., M. R. Raupach, J. G. Canadell, and G. Marland (2009), Trends in the sources and sinks of carbon dioxide, *Nature Geoscience*, *2*, 831–837.

Lee, M., D. P. Marshall, and R. G. Williams (1997), On the eddy transfer of tracers: Advective or diffusive?, *J. Marine Res.*, *55*, 483–505.

Lee, M.-M., and R. G. Williams (2000), The role of eddies in the isopycnic transfer of nutrients and their impact on biological production, *Journal of Marine Research*, *58*(6), 895–917.

Lee, M.-M., A. G. Nurser, A. Coward, and B. De Cuevas (2007), Eddy advective and diffusive transports of heat and salt in the southern ocean, *Journal of physical oceanography*, *37*(5), 1376–1393.

Lumpkin, R., and K. Speer (2007), Global meridional overtuning, *J. Phys. Oceanogr.*, *37*, 2550–2537.

Marshall, J., and T. Radko (2003), Residual mean solutions for the antarctic circumpolar current and its associated overturning circulation, *J. Phys. Oceanogr.*, *33*, 2341–2354.

Marshall, J., and K. Speer (2012), Closing the meridional overturning circulation through Southern Ocean upwelling, *Nature Geoscience*, *5*, 171–180.

Marshall, J., D. Olbers, H. Ross, and D. Wolf-Gladrow (1993), Potential vorticity constraints on the dynamics and hydrography of the Southern Ocean, *J. Phys. Oceanogr.*, *23*, 465–487.

Marshall, J., A. Adcroft, C. Hill, L. Perelman, and C. Heisey (1997a), A finite-volume, incompressible navier stokes model for studies of the ocean on parallel computers, *J. Geophys. Res.*, *102*, 5753–5766.

Marshall, J., C. Hill, L. Perelman, and A. Adcroft (1997b), Hydrostatic, quasi-hystrostatic, and non-hydrostatic ocean modeling, *J. Geophys. Res.*, *102*, 5733–5752.

Marshall, J., E. Shuckburgh, H. Jones, and C. Hill (2006), Estimates and implications of surface eddy diffusivity in the Southern Ocean derived from tracer transport, *J. Phys. Oceanogr.*, *36*, 1806–1821.

Mazloff, M., P. Heimbach, and C. Wunsch (2010), An eddy permitting Southern Ocean state estimate, *J. Phys. Oceanogr.*, *40*, 880–899, in Preparation.

Meredith, M. P., A. C. Naveira Garabato, A. M. Hogg, and R. Farneti (2012), Sensitivity of the overturning circulation in the Southern Ocean to decadal changes in wind forcing, *J. Phys. Oceanogr.*, *42*, 99–110.

Nakamura, N. (1996), Two-dimensional mixing, edge formation, and permeability diagnosed in an area coordinate, *J. Atmos. Sci.*, *53*, 1524–1537.

Naveira-Garabato, A. R., R. Ferrari, and K. Polzin (2011), Eddy stirring in the Southern Ocean, *J. Geophys. Res.*, *116*, C09,019.

Nikurashin, M., and G. Vallis (2012), A theory of the interhemispheric meridional overturning circulation and associated stratification, *J. Phys. Oceanogr.*, *42*, 1652–1667.

Pradal, M.-A., and A. Gnanadesikan (2014), How does the redi parameter for mesoscale mixing impact global climate in an earth system model?, *Journal of Advances in Modeling Earth Systems*, *6*(3), 586–601, doi:10.1002/2013MS000273.

Prather, M. J. (1986), Numerical advection by conservation of second-order moments, *J. Geophys. Res.*, *91*(D6), 6671–6681.

Redi, M. (1982), Oceanic isopycnal mixing by coordinate rotation, *J. Phys. Oceanogr.*, *12*, 1154–1158.

Sabine, C. L., R. A. Feely, N. Gruber, R. M. Key, and et al. (2004), The oceanic sink for anthropogenic co2, *Science*, *305*, 367–371.

Sen, A., R. B. Scott, and B. K. Arbic (2008), Global energy dissipation rate of deep-ocean low-frequency flows by quadratic bottom boundary layer drag: Computations from current-meter data, *Geophys. Res. Lett.*, *35*, L09,606.

Shuckburgh, E., and P. Haynes (2003), Diagnosing transport and mixing using a tracer-based coordinate system, *Physics of Fluids*, *15*(11), 3342–3357.

Smith, K. S., and J. Marshall (2009), Evidence for enhanced eddy mixing at mid-depth in the Southern Ocean, *J. Phys. Oceanogr.*, *39*, 50–69.

Spence, P., O. A. Saenko, M. Eby, and A. J. Weaver (2009), The Southern Ocean overturning: Parameterized versus permitted eddies, *J. Phys. Oceanogr.*, *39*, 1634–1652.

Stammer, D. (1997), Global characteristics of ocean variability estimated from regional TOPEX/ POSEIDON altimeter measurements, *J. Phys. Oceanogr.*, *27*, 1743–1769.

Thompson, A. F., and J.-B. Sallée (2012), Jets and topography: Jet transitions and the impact on transport in the Antarctic Circumpolar Current, *J. Phys. Oceanogr.*, *42*, 956–972.

Toggweiler, J. R. (2009), Shifting westerlies, *Science*, *232*, 1434–1435.

Toggweiler, R., and J. Russell (2008), Ocean circulation in a warming climate, *Nature*, *451*, 286–288.

Treguier, A. M., and J. C. McWilliams (1990), Topographic influences on wind-driven, stratified flow in a beta-plane channel: An idealized model for the antarctic circumpolar current, *J. Phys. Oceanogr.*, *20*(3), 321–343.

Viebahn, J., and C. Eden (2010), Toward the impact of eddies on the response of the Southern Ocean to climate change, *Ocean Modelling*, *34*, 150–165.

Viebahn, J., and C. Eden (2012), Standing eddies in the meridional overturning circulation, *J. Phys. Oceanogr.*, *42*, 1486–1508.

Vollmer, L., and C. Eden (2013), A global map of mesoscale eddy diffusivities based on linear stability analysis, *Ocean Modelling*, *72*, 198–209.

Wright, C., R. B. Scott, B. K. Arbic, and D. G. Furnival (2012), Ocean-eddy dissipation estimates at the atlantic zonal boundaries., *J. Geophys. Res.*, *117*, C03,049.

Wright, C. J., R. B. Scott, D. Furnival, P. Ailliot, and F. Vermet (2013), Global observations of ocean-bottom subinertial current dissipation, *J. Phys. Oceanogr.*, *43*, 402–417.

Waugh, D., Changes in the ventilation of the southern oceans, *Phil. Trans. R. Soc. A*, *372*, 20130,269, 2014.

Waugh, D., F. Primeau, T. DeVries, and M. Holzer, Recent changes in the ventilation of the southern oceans, *Science*, *339*, 568–570, 2013.

Rintoul, S. R., and A. C. Naveira Garabato, Chapter 18 - dynamics of the southern ocean circulation, in *Ocean Circulation and Climate: A 21st Century Perspective*, *International Geophysics*, vol. 103, edited by J. G. Gerold Siedler, Stephen M. Griffies and J. A. Church, pp. 471 – 492, Academic Press, 2013.

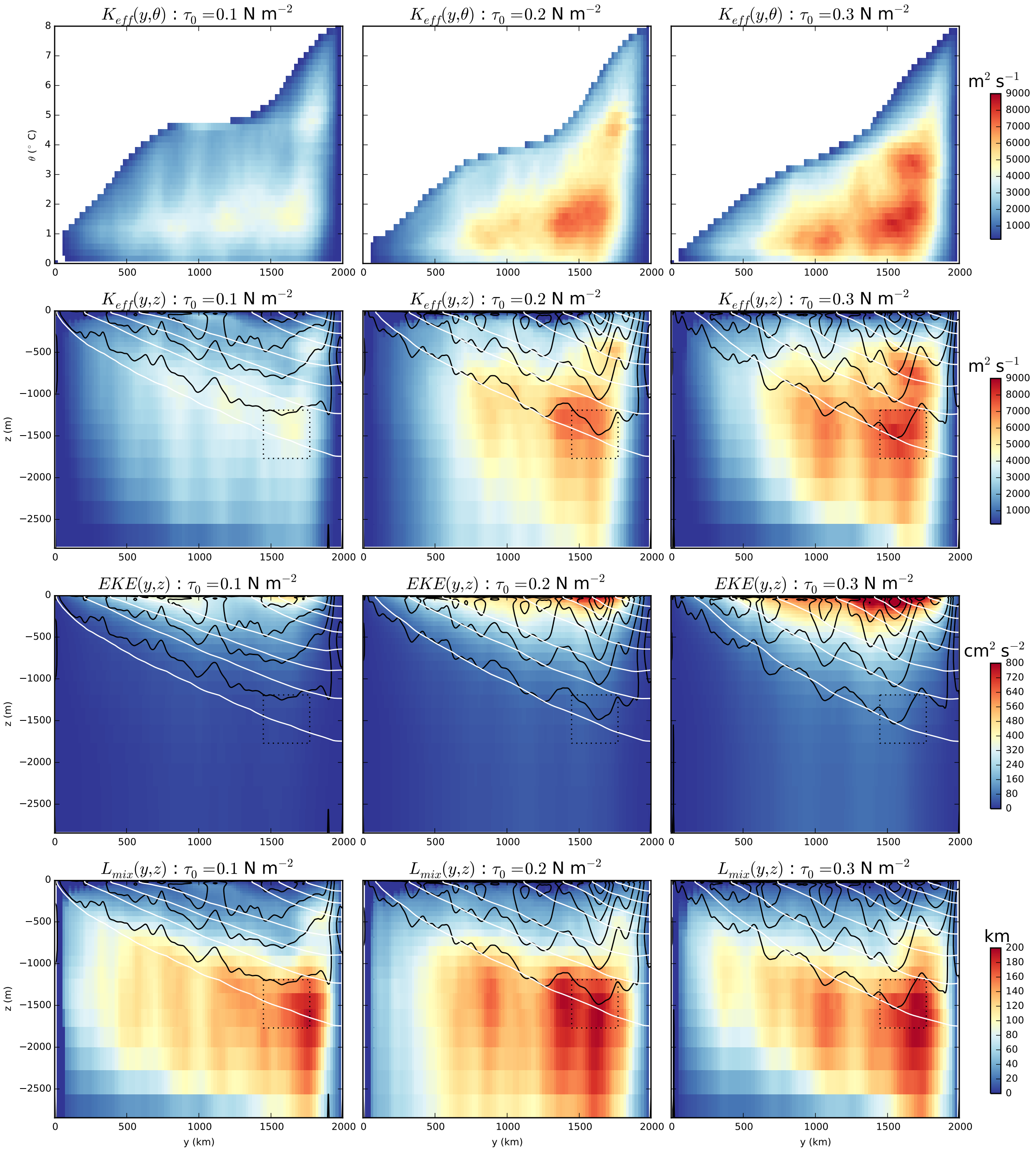

Figure 1. First row: K_{eff} in temperature coordinate for different values of wind strength. Second row: K_{eff} interpolated to depth coordinate. The white contours are isotherms and the black contours are isotachs of the zonal mean flow. Third row: zonal mean eddy kinetic energy. Fourth row: effective mixing length. The dotted-line box shows the region where the averages are taken to produce Fig. 2

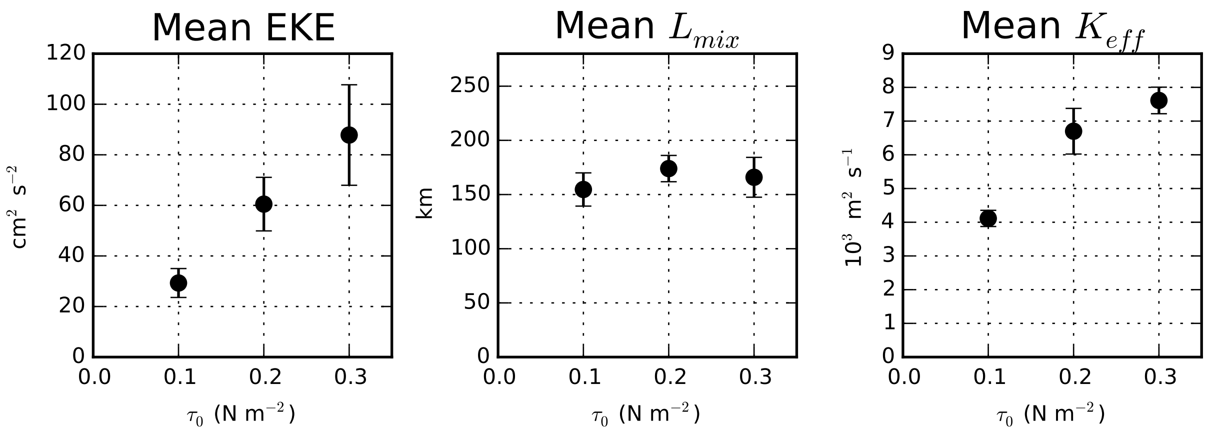

Figure 2. Average values of EKE, K_{eff} and L_{mix} from the boxed region indicated in Fig. 1. The error bars show the standard deviation for the spatial average.

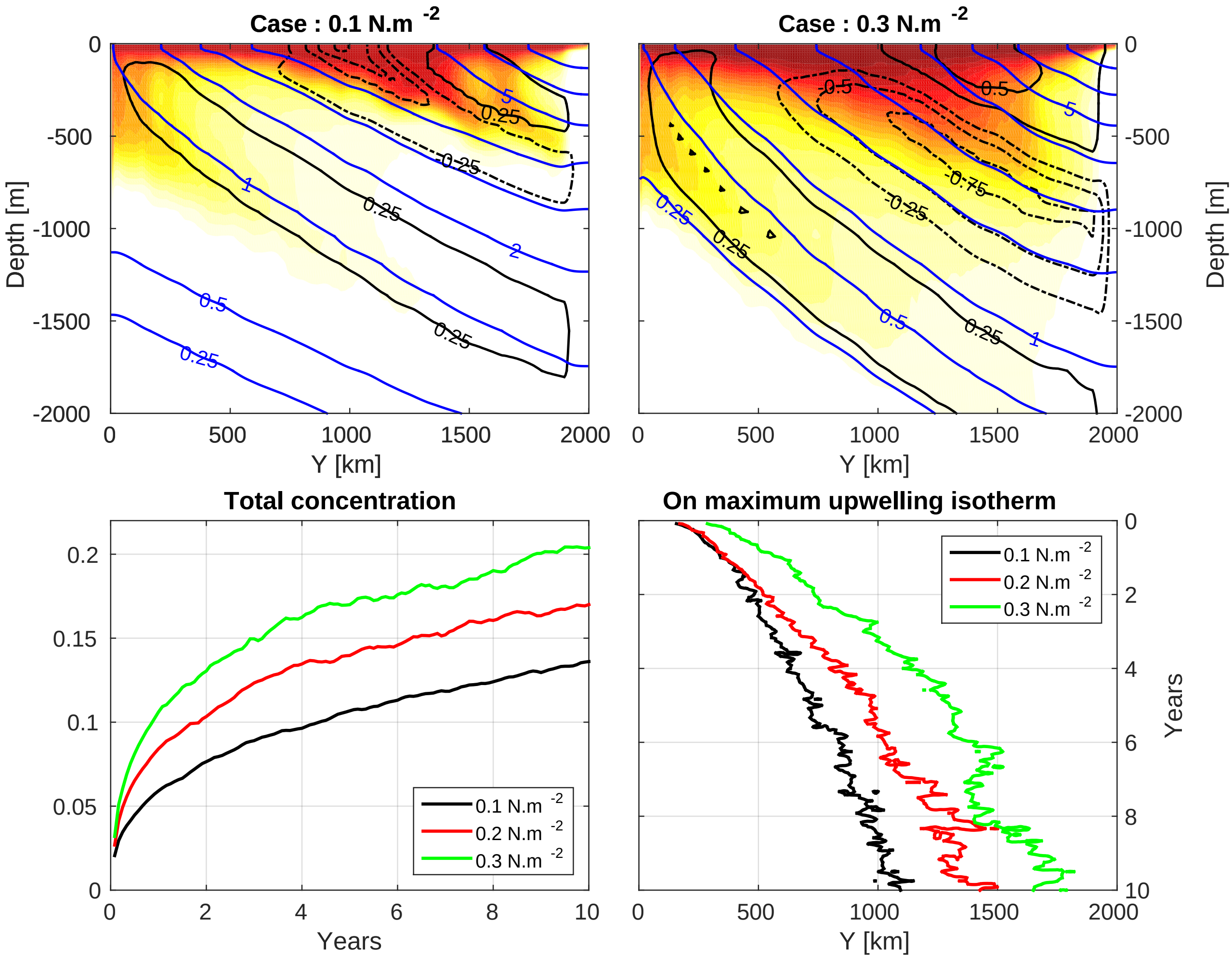

Figure 3. Top row: Distribution of the ventilation tracer after 5 years for wind stress τ_x=0.1 N m^{-2} (left) and 0.3 N m^{-2} (right). The time mean isotherms and residual-mean MOC are shown in blue and black contours respectively (solid for clockwise, dashed for anti-clockwise). Bottom row: (left) Time evolution of the globally averaged tracer concentration for the three wind magnitudes. (right) Meridional location of the 0.1 unit/m^3 tracer value on the isotherms of maximum upwelling (1.5, 1.1 and 0.9 °C for τ_x=0.1, 0.2, and 0.3 N.m^{-2}, respectively).